

Shearing Capacity and Adhesive Properties of Reinforced Interface for RC Beam with Haunch Retrofitted by CFRP Grid with Spraying PCM Shotcrete

by

Rui GUO^{*}, Kohei YAMAGUCHI^{**}, Shinichi HINO^{***} and Nobuhiro MIYANO[†]

(Received July 14, 2014)

Abstract

In this study, the effect of shearing capacity of RC beams with haunch by PCM shotcrete method with CFRP grid was examined. It was carried out 3 standards as a parameter with the reinforced quantity of CFRP grid. There were 5 type specimens: Unreinforced RC Beam (P-1), Reinforced RC Beam which was reinforced by PCM only (P-2), Reinforced RC Beams which was reinforced by PCM and CFRP grid (CFRP grid type: CR-4, 6 and 8) (P-3, 4, 5). The reinforced range of beams was web and haunch. Also, in order to clarify the adhesive properties of the reinforced interface between PCM and existing concrete, it was investigated by FEM analysis.

Keywords: CFRP grid, PCM shotcrete method, Shearing capacity, FEM analysis, Adhesive properties

1. Introduction

In the Great East Japan Earthquake in 2011, the shear failure of many underground structures, such as RC structures which were designed and constructed by old design standards, was confirmed. In this study, it was intended for sluice(**Photograph1**¹⁾), which is an important structure placed across a river embankment to be used to drain waste water from protected inland and pump water from river, among the underground structures. In addition, the sluice pipe body partition was catastrophic destroyed in major earthquakes. It was pointed that the shear reinforced in the plane of the partition wall was needed due to uneven settlement of sluice. The shear reinforced amount of the partition wall designed in the former standard was insufficient. In the case that the conventional method was required to drilling the haunch both web sides, the reinforcement was inserted therein. However, since the rebar in haunch was dense, it was difficult to drill the haunch in actual construction. Also, in order to prevent corrosion measures of reinforcement, increased thickness of the site affected by the water was generally about 250mm. The inhibition rate of the cross section

* Graduate Student, Department of Urban and Environmental Engineering

** Assistant Professor, Department of Civil Engineering

*** Professor, Department of Civil Engineering

† Repair Division, SNC Co.Ltd., Japan

was too large. In consideration of these things, Carbon Fiber Reinforced Plastic (CFRP grid (**Photograph2**)), which was fixed with other materials easily and had good corrosion resistance, was used to instead of the rebar. Shear reinforced method of RC beam by CFRP grid spraying Polymer Cement Mortar (PCM) shotcrete method was developed. The benefits of this method are unnecessary to drill the haunch, increased thickness amount is thinner, and corrosion resistance is improved by CFRP grid.

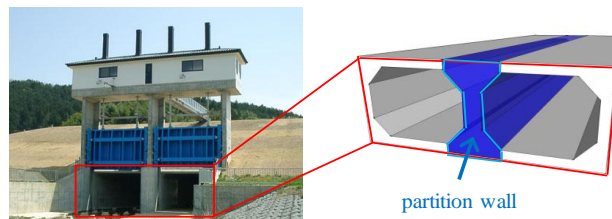
It was not clarified the effect of shearing capacity of RC beams with CFRP grid spraying PCM shotcrete by Bond-slip Behavior of Two Dimensional Carbon Fiber-reinforced Plastic Grids²⁾ and The Strengthening Effect of Damaged RC Beams by Attaching the Lattice-form CFRP with a Joint and Scotcreting of the Polymer Mortar³⁾. Thus, in previous studies⁴⁾, it was carried out by comparing with two kinds of RC beams, one was reinforced by PCM and CFRP grid fixed with only web, and the other was fixed with web and haunch. It was seen that the shearing force was resisted by the shear reinforcement setting up in concrete, and CFRP grid. The effect of shear reinforced of RC beams had been confirmed. In particularly, in the beam which was reinforced by PCM and CFRP grid fixed with web and haunch, the integrity of the reinforced section and the existed section was good. The effect of shear reinforced was sufficient. However, for the size of specimens was about 1/3~1/4 corresponds to that of actual structures, (height of haunch of real structure: 200~300mm, height of haunch of specimens: 75mm), There were 2 grid points being fixed in haunch. The stress transferring mechanism of out-of-plane fixation was unknown, and the calculation method for shear strength according to the amount of CFRP grid had not been established.

In order to study the effect of shearing capacity, it was carried out 3 standards as a parameter with the reinforced amount by experiment and FEM Analysis. Also, in order to reveal adhesive properties of the reinforced section interface of PCM and existing concrete, it was investigated by FEM analysis.

2. Loading Experiment and FEM Analysis Description

2.1 Specimens

In previous studies on adhesive properties of reinforced section interface⁵⁾, it was found that when the load occurred to 2/3 of the design tensile strength of the grid, in order to ensure the distribution ratio of grid was over 90%, the number of grid point was 3 or more. Thus, the size of haunch of specimens was the same as the actual structures to secure, and there were 4 grid points being fixed in haunch of specimens. Specimens were I digit, simulating the existing structures RC



Photograph1 Sluice¹⁾.



Photograph2 CFRP grid.

beam, with span length of 4750mm and cross-sectional dimension of 750mm×500mm (width × height). Specimens were produced by five types: unreinforced beam (P-0), reinforced beam which was reinforced by PCM only (P-1), reinforced beams which were reinforced by PCM and CFRP grid (CFRP grid type: CR-4, 6, 8) (P-2, 3, 4). The reinforced range of beams was web and haunch.

The shapes of specimens and the situation of reinforcement and CFRP grid were shown in **Fig.1**. The Ordinary Portland Cement (OPC, density: 3.14 g/cm³), sea sand (density: 2.59 g/cm³) as fine aggregate, crushed stone (density: 2.76 g/cm³) as coarse aggregate were used in concrete mixture.

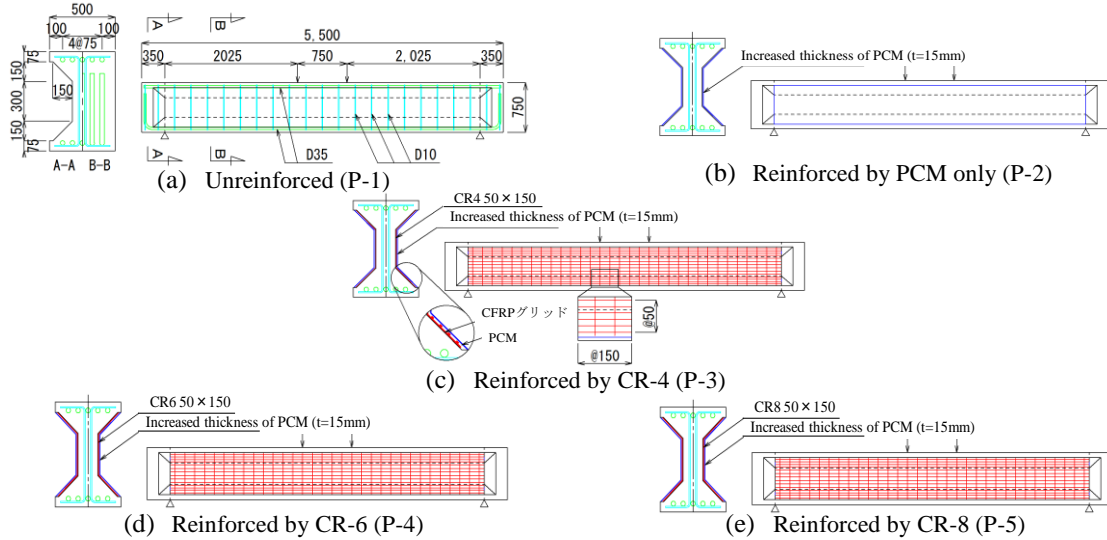


Fig.1 Schematic of Specimens.

Table 1 Proportion of Concrete.

G _{max} (mm)	W/C (%)	s/a (%)	Unit Amount (kg/m ³)						
			W	C	S1	S2	G1	G2	Ad
20	63	45.8	170	270	578	250	747	308	2.7

G_{max}: The Maximum Size of Coarse Aggregate, W: Water, C: Cement, s/a: Sand Percentage
 S: Fine Aggregate, G: Coarse Aggregate, Ad: AE Water Reducing Agent.

Table 2 Material Properties for Concrete and PCM.

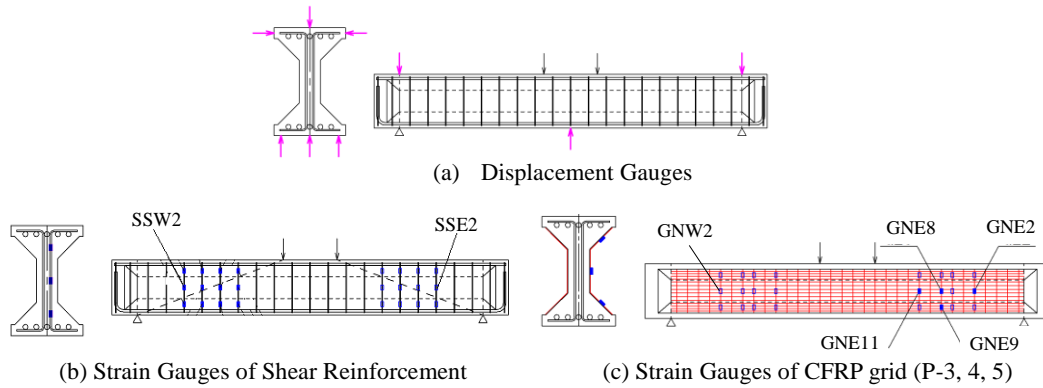
Type	Material	-	Compressive Strength (N/mm ²)	Flexural Strength (N/mm ²)	Tensile Strength (N/mm ²)	Young's Modulus (×10 ⁴ N/mm ²)
P-1,2	Concrete	Design Value	21.0	3.20	-	2.35
		Actual Value	23.9	3.43	2.07	2.35
	PCM	Design Value	69.9	9.00	3.16	2.70
		Actual Value	54.3	9.4	-	2.45
P-3,4,5	Concrete	Design Value	21.0	3.20	-	2.35
		Actual Value	24.5	3.71	2.09	2.50
	PCM	Design Value	69.9	9.00	3.16	2.70
		Actual Value	51.9	7.4	-	2.45

Table 3 Material Properties for Reinforcement.

Rebar Diameter	Materials	Yield Strength (N/mm ²)	Tensile Strength (N/mm ²)	Young's Modulus ($\times 10^5$ N/mm ²)
D35	Longitudinal Reinforcement	381	549	2.00
D10	Shear Reinforcement	397	523	

Table 4 Material Properties for CFRP Grid.

Grid Type	Cross-sectional Area (mm ²)	Tensile Strength (N/mm ²)	Young's Modulus ($\times 10^5$ N/mm ²)
CR-4	6.6	1400	1.00
CR-6	17.5		
CR-8	26.4		

**Fig.2** Installed Position of Displacement Gauges and Strain Gauges.

AE water reducing agent was used as the admixtures. Proportion of concrete was shown in **Table 1**. The material properties for concrete, PCM, reinforcement and CFRP grid were shown in **Table 2, 3, 4**. The material properties for reinforcement and CFRP grid were test values.

2.2 Method of Experiment

The position of the measuring equipment was shown in **Fig.2 (a)**. Loading was set in two-point in shear span length of 2025mm as a simply support at both ends, loaded in a uniform rate. The displacement gauges were placed on three locations width direction of span center bottom edge of beams, and displacement of the supporting points was also measured. In the axial direction of the beam, strain gauges were attached on the span central upper edge of the concrete, tension side of rebar and CFRP grid. In the shear direction of the beam, In order to study on the effect of shear reinforced of RC, for the strain values of CFRP grid were particularly important, so strain gauges of shear reinforced of reinforcement and CFRP grid were measured at a plurality of locations, which were shown in **Fig.2 (b), (c)**.

2.3 FEM Analysis

FEM Analysis was performed in three-dimensional nonlinear analysis, using generic FEM software Diana. The boundary conditions were supported at fulcrum positions by using truss

element, and the loading conditions were made a forced displacement in vertical direction by using used curve shell element. Concrete and PCM used Solid Elements, reinforcement and CFRP grid used Bar Elements. One example of analysis models was shown in **Fig.3**. The constitutive laws of concrete and PCM, reinforcement and CFRP grid used in FEM Analysis were shown in **Fig.4, 5, 6**. The base function in compression of concrete and PCM, with the parameters stress and strain, was modeled with a number of different predefined and user-defined curves. And the curve was according to the Thorenfeldt⁶⁾ and the parabolic curve, which is a formulation based on fracture energy, according to Feenstra⁷⁾, in DIANA. The compressive side of the constitutive laws of concrete and PCM were based on the results of strength test, the tensile side was applied the tensile softening curve proposed based on Standard Specifications for Concrete Structures⁸⁾. The constitutive law of reinforcement was applied the yield condition of Von Mises, it increased in linear until yield strength, thereafter stress constant strain increased as a bilinear mode. The constitutive law of CFRP grid was stress and strain became to zero after reaching the yield strength.

In order to model the adhesive properties of the reinforced interface, Interface Elements were used at the interface of the PCM and existing concrete. The Sliding relationship was defined in **Fig.7** that was applied from DIANA user manual of adhesive properties for concrete-concrete. The relationship between stress-relative displacement in tangential direction of interface between PCM and existing concrete was shown in **Fig.7 (a)**, and the relationship in normal direction was shown in **Fig.7 (b)**. The red line shown in **Fig.7 (a)** was defined the sliding relationship of P-2, which was reinforced by PCM only. And the black line was defined the sliding relationship of P-3, 4, 5, which were reinforced by PCM and CFRP grid. The initial slope of black line is 10 times to the red line.

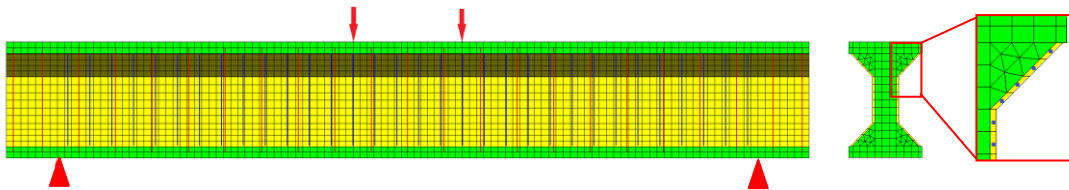


Fig.3 FEM Analysis Model (Reinforced Beam reinforced by PCM and CFRP grid).

G_F : Fracture Energy (N/m), f'_c : Compressive Strength (N/mm²),

f_{tk} : Tensile Strength (N/mm²), d_{max} : Maximum Dimensions of Coarse Aggregate (mm)

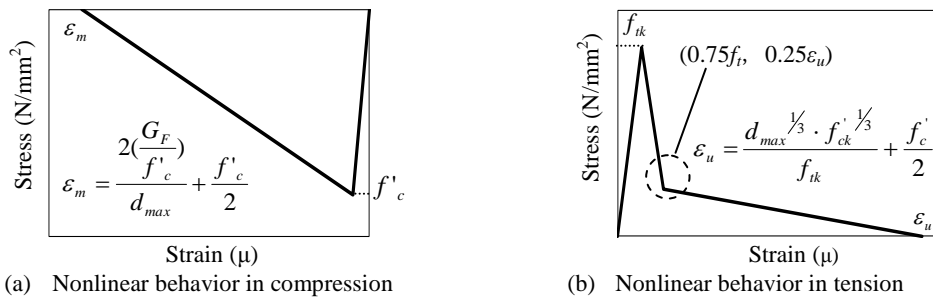


Fig.4 Constitutive Laws of Concrete and PCM.

f_y : Yield Strength (N/mm²), ϵ_y : Yield Strain of Reinforcement (μ)
 f_t : Tensile Strength (N/mm²), ϵ_t : Yield Strain of CFRP Grid (μ)

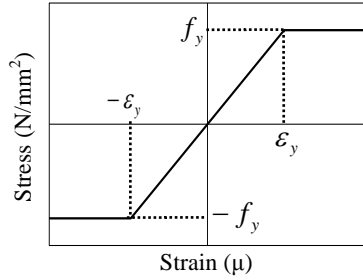


Fig.5 Constitutive Laws of Reinforcement.

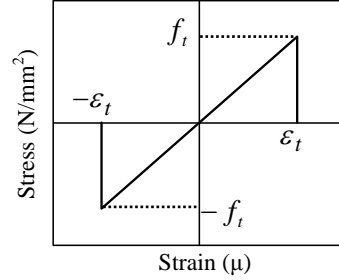
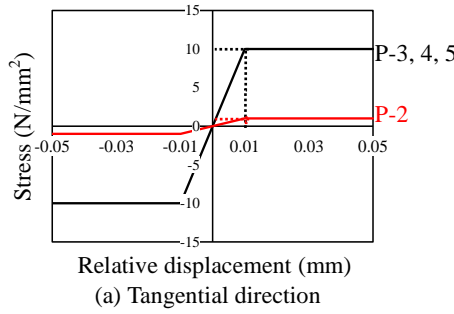
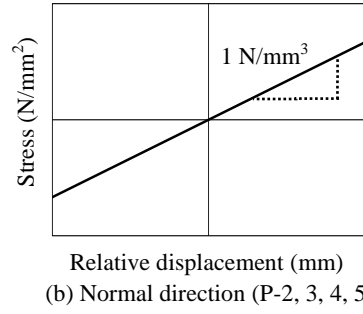


Fig.6 Constitutive Laws of CFRP grid.



(a) Tangential direction



(b) Normal direction (P-2, 3, 4, 5)

Fig.7 Adhesive Properties.

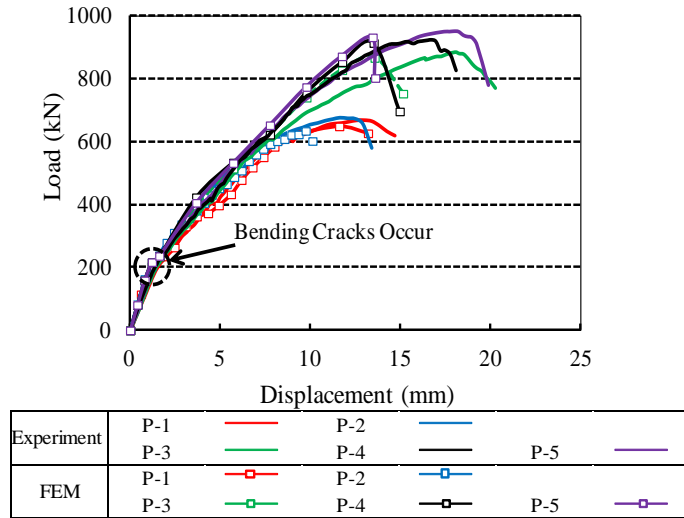


Fig.8 Load-Deflection Curve.

3. Results and Discussion

3.1 Relationship of Load-Deflection

Relation of Load-deflection was shown in **Fig.8**. Failure Pattern of specimens was shear failure. It was seen that the maximum load of P-1 (unreinforced beam) and P-2 (reinforced by PCM only) were almost the same, and the contribution of shear strength according to PCM was few. The maximum loads of P-3, 4, 5 (CR-4, 6, 8) were improved by 30-40% comparing to P-1, 2. Among the reinforced beams which were reinforced by CFRP grid, the maximum loads of P-4, 5 (CR-6, 8) were improved by about 7% comparing to P-3 (CR-4). At about 200kN, bending cracks were

observed on the surface of specimens. In FEM Analysis, the maximum loads of specimens and the change of stiffness were possible to be reproduced, and shear failure was also exhibited.

3.2 Load-Strain of Shear Reinforcement Relation

Load-Strain of shear reinforcement was shown in Fig.9. The strain of CFRP grid of P-3, 4, 5 were also considered. In unreinforced type P-1, it was seen that the obliquely shear cracks were confirmed in the surface of specimen at about 400kN during the experiment. The strain of shear reinforcement also increased at the same time, and then it was failure in the end. Further, in P-2, which was reinforced by PCM only, it was seen that the behavior was similar to the unreinforced beam P-1. In P-3, 4, 5, the strain of CFRP grid and shear reinforcement showed almost the similar behavior, which increased gradually until reaching the yield strain, than that of P-1, 2. It suggested that the shear forces were resisted by CFRP grid and shear reinforcement, which were integral. In FEM Analysis, because the model is symmetrical, the values of strain in eastern and western considered position are almost the same, so the results of FEM analysis are average value.

3.3 Cracks Pattern

The properties of cracks in experiment and FEM Analysis at maximum load were, and the properties of cracks of P-3, 4, 5 (CR-4, 6, 8) in FEM Analysis at about 850kN were shown in Table 5. During the experiment, the small width flexural cracks occurred at loading position firstly. Then the obliquely shear cracks occurred on the line connecting the loading position and beam support. When the load increased, the length and width of cracks developed. Finally, part of the upper edge of concrete was crushed.

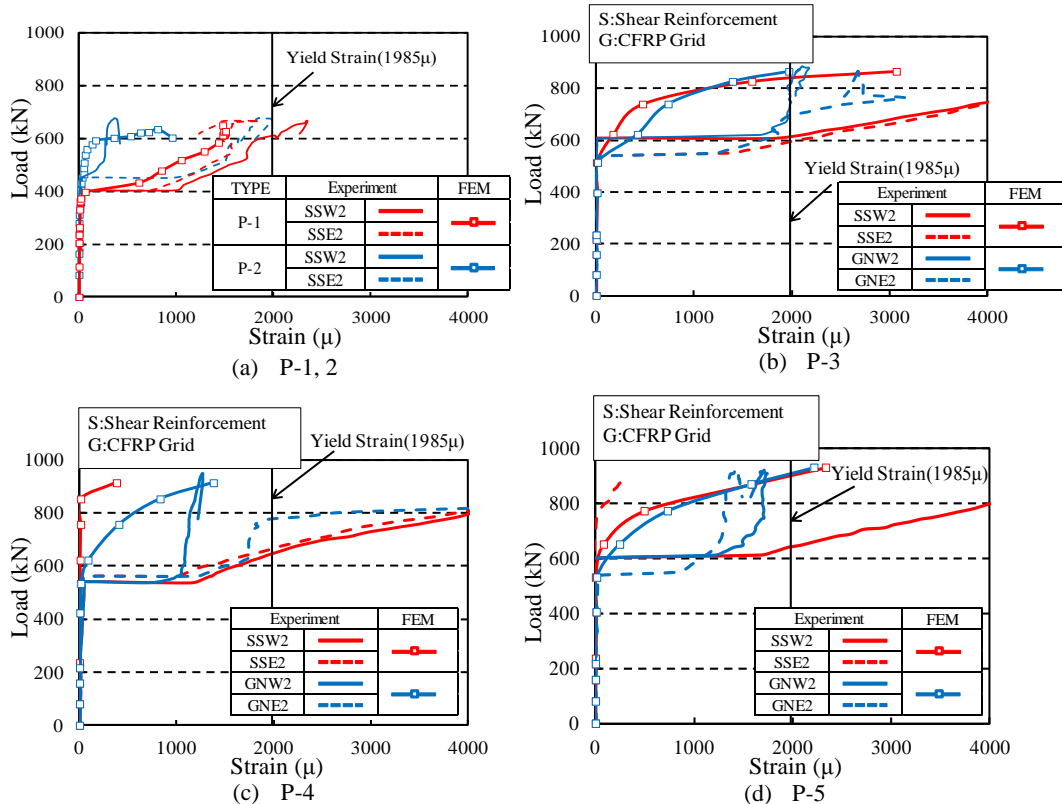
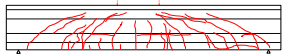
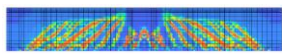

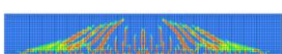
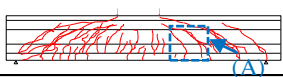
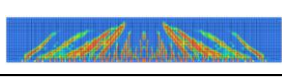
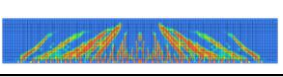

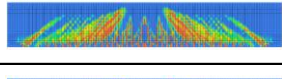
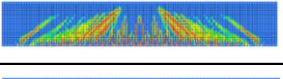

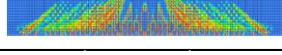
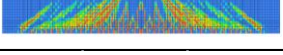
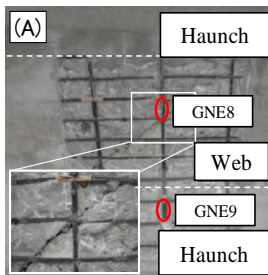


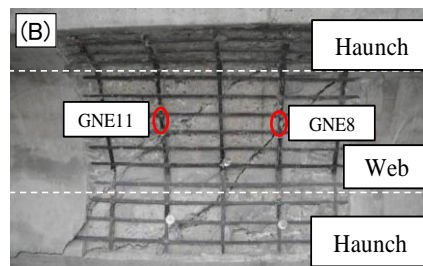
Fig.9 Load-Strain of Shear Reinforcement.

Table 5 Cracks Pattern.

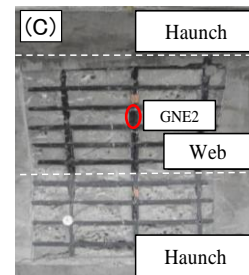
TYPE	At Maximum Load		At 850kN
	Experiment	FEM	FEM
P-1			-
P-2			-
P-3			
P-4			
P-5			



(a) P-3



(b) P-4



(c) P-5

* Considered positions were shown in **Fig.2** (c)

Photograph3 Situations of CFRP grid.

In P-3, 4, 5 (CR-4, 6, 8), compared with each other, it was seen that the width of cracks is larger as the cross-sectional area of CFRP grid is smaller. However, in P-5(CR-8), more cracks occurred than other specimens, since the rigidity of CFRP grid was high. In addition, the trend of cracks was shown in FEM at the same load (850kN), the stress was larger as the cross-sectional area of the CFRP grid is smaller. The principal stress contour was generally similar to the results of experiments.

The failure situations of PCM and breaking situations of CFRP grid were confirmed after experiment, and the results were shown in **Photograph3**. In P-3 (CR-4), the breaking of CFRP grid cannot be seen near the locations of strain gauges. It was observed that the orthogonality of grid rated section above the shear cracks was lost, and the breaking location was confirmed. In addition, the breaking of CFRP grid cannot also be seen in P-4, 5 (CR-6, 8). Further, there wasn't any separation between existing concrete and PCM.

3.4 Adhesive Properties of Interface of Reinforced Section

In order to clarify the adhesive properties of the reinforced interface of PCM and existing concrete, it was investigated by comparing with the relative displacement in tangential section (in-plane) of P-2 (PCM only) and P-3 (CR-4) by FEM analysis. The considered position of relative displacement and the relationship of Load-Relative Displacement were shown in **Fig.10** and **Fig.11**. In the web (W), at about 300kN, the relative displacement of P-2 (PCM only) was rapidly increasing, it was reproduced that the interface between PCM and existing concrete was peeled off.

In P-3 (CR-4) , the relative displacement occurred slightly finally, this is because of the destruction of PCM and concrete. In the comparison of P-2 (PCM only) and P-3 (CR-4) in the haunch (H), the relative displacement of P-2 (PCM only) increased in a linear fashion from low load, and soared finally. On the other hand, the relative displacement of P-3 (CR-4) did not rapidly increase until the ultimate time. It was seen that the adhesive properties of the reinforced section interface and the failure behavior of CFRP grid were possible to reproduce.

3.5 Evaluation of Shearing Capacity

The comparison of shearing capacity was shown in **Table 6**. Design.1 can be calculated by in **Equations (1)**⁸⁾. The shearing capacity of CFRP grid was shown in **Equations (2)**, in the case that $\epsilon_{fwd}=14000\mu$ (failure strain of CFRP grid). The ratio of design value and test value was higher than 1.00 in P-1, P-2 and P-3. It can be evaluated on the safe side. However, in P-4, P-5, the ratio of the design value and test value was below 1.00, it was assessment of risk side.

The distributions of the maximum value of strain of CFRP grid at each measurement position were shown in **Fig.12**. It was seen that when the shear destruction occurred, the strain of CFRP grid was smaller than the failure strain (14000μ). The relationship between the cross-sectional area and strain of CFRP grid setting in the shear direction was shown in **Fig.13**. It was seen that the test value (the average of maximum strain of CFRP grid), effective strain of CFRP grid were almost the same. FEM value was a little smaller than the test value.

However, it can be seen from **Fig.12**, strain of many locations were in $6000-10000\mu$. In order to evaluate the shearing capacity, as the separation between concrete and PCM, the failure strain of CFRP grid did not reach. Design.2 was applied the concept of effective strain of CFRP grid⁹⁾. Thus, the shearing capacity was shown in **Equations (2), (3) and (4)**. In all specimens, the ratio of design value and test value became higher than 1.00. It was seen that the evaluation of shearing capacity was in the safety side. The ratio of Design.2 value and test value of P-3, P-4, P-5 (CR-4, 6, 8) was higher than that of P-1 (unreinforced specimen), it was obtained that the reinforced effect of RC beams, which were reinforced by CFRP grid, was sufficient. Thus, since the ratio of design value and test value of unreinforced specimen (P-1) was 1.31. Effective strain of P-3, P-4, P-5 (CR-4, 6, 8), in the case the the ratio was also 1.31, were also shown in **Fig.13**. It was seen that the smaller cross-sectional area of CFRP grid was, the effective strain calculated from experiments increased.

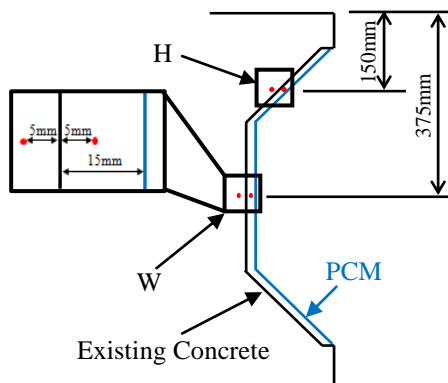


Fig.10 Considered Position of Relative Displacement.

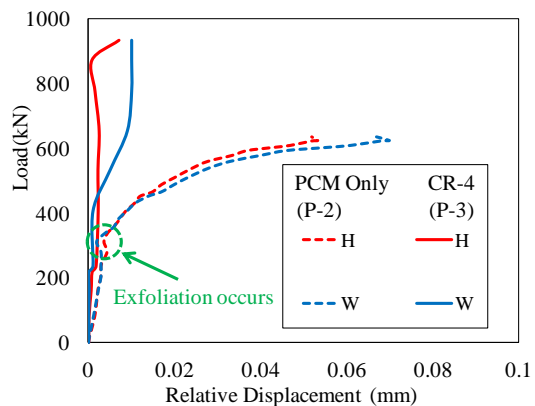
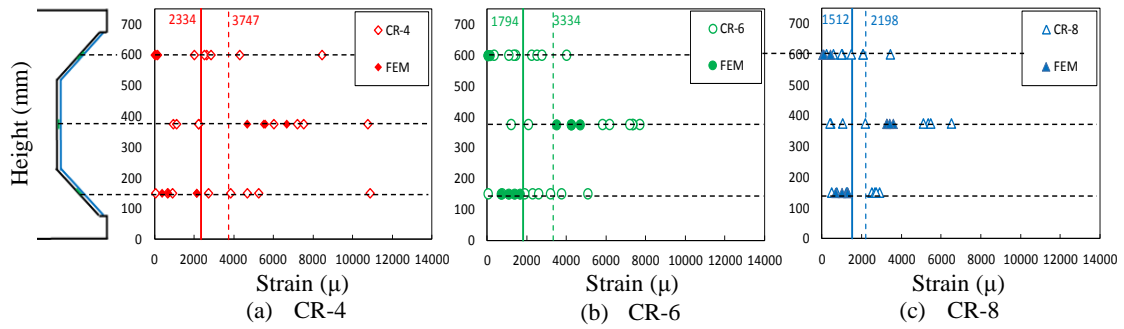


Fig.11 Load- Relative Displacement.

Table 6 Comparison of Shear Capacity.

TYPE	Design 1	Design 2	Experiment	FEM	Exp /Design 1	Exp /Design 2	Exp /FEM
P-1 (Unreinforced)	509	-	665	649	1.31	-	1.02
P-2 (PCM Only)	548	-	677	634	1.24	-	1.07
P-3 (CR-4)	715	629	885	866	1.24	1.41	1.02
P-4 (CR-6)	998	676	949	914	0.95	1.40	1.04
P-5 (CR-8)	1230	698	922	932	0.75	1.32	0.99

**Fig.12** Distribution of Strain of CFRP grid.

$$V = V_{con} + V_{pcm} + V_{st} + V_G \quad (1)$$

V_{con} : Share of the Shearing Capacity of Concrete (kN),

V_{pcm} : Share of the Shearing Capacity of PCM (kN),

V_{st} : Share of the Shearing Capacity of Shear Reinforcement (kN),

V_G : Share of the Shearing Capacity of CFRP Grid (kN).

Where,

$$V_G = A_W \cdot E_W \cdot \varepsilon_{fwd} (\sin \alpha_s + \cos \alpha_s) / S_S \cdot z / \gamma_b, \quad (2)$$

$$\varepsilon_{fwd} = [f'_{mcd} p_w E_{fu} / (p_{web} E_w)]^{0.5} \times 10^{-4}, \quad (3)$$

$$f'_{mcd} = f'_{cd} \cdot (h/0.3)^{-0.1}, \quad (4)$$

$$p_w = A_S / (b_w d), \quad p_{web} = A_W / (b_w S_S),$$

ε_{fwd} : Effective Strain, d : Effective Height (mm),

E_W : Young's Modulus of Grid (N/mm²),

A_W : Total Cross-Sectional Area of CFRP Grid in the Interval S_S (mm²),

S_S : Arrangement Interval of CFRP Grid (mm),

E_{fu} : Young's Modulus of Tensile Reinforcement (N/mm²),

A_S : Cross-Sectional Area of the Main Reinforcement (mm²),

b_w : Width of Abdomen (mm)

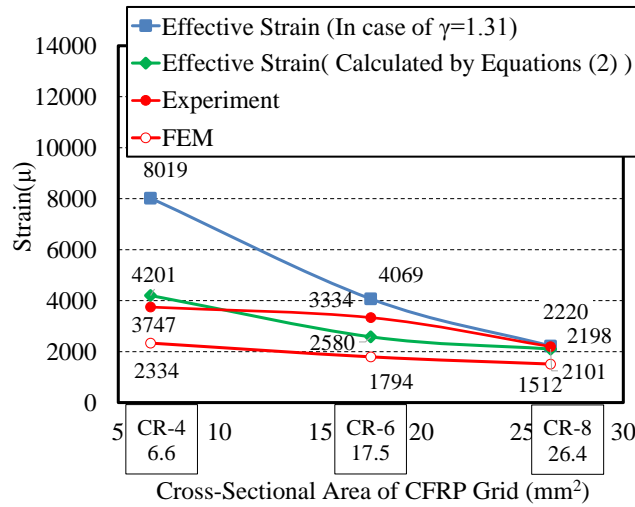


Fig.13 Relationship between Strain and Cross-Sectional Area of CFRP grid.

4. Conclusion

- (1) It was obtained that the reinforced effect of RC beams, which were reinforced by CFRP grid, was sufficient.
- (2) The effective strain of CR-4 was larger than that of CR-6, 8, and the cross-sectional area of CFRP grid of CR-4 was the smaller than that of CR-6, 8. It was considered that the smaller the cross-sectional area of the CFRP grid was, the better capability of deformation was.
- (3) It was clarified that the relative displacement of P-2, which was reinforced by only PCM, increased rapidly, and the interface between PCM and existing concrete was peeled off.
- (4) Comparing with P-2, the adhesive properties of reinforced section interface of P-3, which was reinforced by PCM and CFRP grid, was improved. It was clarified that fixing force was adequate.
- (5) It was clarified that the shearing capacity obtained in the case that the maximum strain of the CFRP grid was failure strain (14000μ), it can be evaluated on the safe side in P-1, P-2 and P-3. However, the evaluation of shearing capacity in P-4 and P-5, it was assessment of risk side.
- (6) It was clarified that the evaluation of shearing capacity, which was used the concept of effective strain, was in the safety side. It is possible to evaluate the shearing capacity by using the concept of effective strain.

Acknowledgements

This work was supported by JSPS KAKEN; Grant-in-Aid for Scientific Research (A) Number 24246080 and FRP Grid Method Association/ Polymer Cement Mortar Shotcrete Association.

References

- 1) www.sanyukogyo.co.jp
- 2) Ichiro KURODA, Takayuki NAGAHAMA, Shinichi HINO, Toshiaki OHATA; Bond-slip Behavior of Two Dimensional Carbon Fiber Reinforced Plastic Grids, Concrete Research and Technology, Vol.12, No.3, pp.69-78 (2001) [in Japanese].
- 3) Satou KOUICHI, Otagiri YOSHIHARU, Tsuji YUKIKAZU, Okamura YUUKI; The

- Strengthening Effect of Damaged RC Beams by Attaching the Lattice-form CFRP with a Joint and Scotcreting of the Polymer Mortar, Proceedings of Annual Conference, V26, No.2, pp.1735-1740 (2004) [in Japanese].
- 4) Nobuhiro MIYANO, Kohei YAMAGUCHI, Suzurishi TANIGUCHI, Shinichi HINO; Shear Reinforcement Effect of RC Beams with CFRP grid by PCM spraying, Proceedings of the Japan Concrete Institute, Vol.35, pp.1423-1428 (2013.7) [in Japanese].
 - 5) Koki SUGIYAMA, Kohei YAMAGUCHI, Satoshi NAKAMURA, Shinichi HINO; Stress Transfer Mechanism of the Reinforced Interface and Seismic Retrofit Existing RC, Journal of Structural Engineering, Vol.57A, pp.1042-1051 (2011.4) [in Japanese].
 - 6) THORENFELDT, E., TOMASZEWICZ, A., JENSEN, J. J; Mechanical Properties of High-Strength Concrete and Applications in Design. Proc. Symp. Utilization of High-Strength Concrete (Stavanger, Norway) (Trondheim, 1987).
 - 7) FEENSTRA, P. H; Computational Aspects of Biaxial Stress in Plain and Reinforced Concrete, PhD thesis, Delft University of Technology (1993).
 - 8) Japan Society of Civil Engineers: Standard Specifications for Concrete Structures (2013.3) [in Japanese].
 - 9) Japan Society of Civil Engineers: Design and Construction Guidelines for Concrete Structures using Continuous Fiber Reinforcement [Design] (1996.9) [in Japanese].